

# Static equilibrium states of von Mises trusses

Zdeněk Kala, Martin Kalina

**Abstract**—The paper deals with the stability problems of steep von Mises trusses with or without influence of initial geometrical imperfections. The complicated nonlinear problem is concerned which was solved by the method form finding. This method seeks an ideal shape of the von Mises truss at displacement of top joint. The paper presents a detailed description of calculation by this method. Applying the method form finding, areas of static equilibrium states of three steep von Mises trusses at displacement of top joint both in vertical and horizontal directions were obtained. The calculation process of these areas, and their drawing are described. These areas are illustrated for the von Mises trusses with influence or without influence of initial curvature of one bar.

**Keywords**—Elastic potential energy, form finding method, static equilibrium states, von Mises truss, buckling, stability.

## I. INTRODUCTION

THE von Mises truss is a simple bar structure consisting of two bars connected by the top joint to each other [1], [2]. The loading action of the top joint can have the form of vertical force or of vertical displacement. The elastic potential energy (further on, potential energy) is changed by loading action, and the stability of von Mises truss is disturbed [3].

The potential energy is the energy which is stored when a body is deformed. In this paper, the use of calculation of potential energy for the stability analysis will be presented. The potential energy of the von Mises truss will be obtained by numerical analysis of the position of each node [4]. In spite of seeming simplicity, the von Mises truss is the subject of permanent scientific interest due to research into types of structural instabilities [5], [6].

The stability of steel bars or beams is a phenomenon connected with buckling or lateral-torsional buckling [7]. The failure mechanism of a steel strut may appear to be a simple topic, but its fundamental has sometimes eluded practitioners and researchers in the field. A steel strut, no matter how slender it is, does not reach its ultimate static resistance (load-carrying capacity) when it buckles elastically, but after the critical cross-section has yielded sufficiently under combined compression and bending [8]. Real steel struts are invariably subject to initial crookedness, so a steel strut typically follows

the path denoted by Curve "Imperfect bar" in Fig. 1. The results of experimental research of load-deflection path were published, e.g., in [9], [10]. Theoretical and experimental research provides important data for sensitivity analyses [11-13], investigation into the reliability of structures [14-16], and for multiple-criteria decision analyses, see, e.g., [17-22].

The consequence of instabilities of high von Mises truss is the fact that the nonlinear finite element solution by the current software is numerically demanding, and need not correspond to the results found experimentally [23]. Generally, the geometrically nonlinear solution based on increasing load action investigates into the increasing path of imperfection beams reliably, see Fig. 1. After having reached the peak, the force decreases, and deformation increases. After having reached the peak, the tangential stiffness matrix of the structure is not positive definiteness, and it can cause the numerical instability of solution.

In the presented paper, the method of dynamic relaxation (form finding) is applied, which showed itself as appropriate for solution of stability types of problems of the von Mises trusses [24]. The method evaluates the potential energy of the system after imposing the control displacement in the set relaxation time. So, the energy stored in the von Mises truss due to elastic deformation of bars, i.e., of their stretching, compression, or bending is obtained. This potential energy in the von Mises truss need not be extreme (minimum), it is generally the potential energy obtained during the relaxation time. By recording the potential energy into the space areas, static equilibrium states (further on, only SES) are obtained [25], [26].

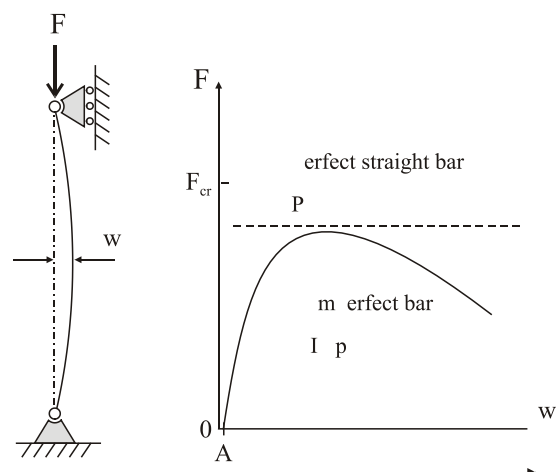


Fig. 1 load-deflection path of perfect and imperfect elastic strut

This result was achieved with the financial support of the Project GAČR 14-17997S and Project no. LO1408 "AdMAs UP".

Zdeněk Kala is with Brno University of Technology, Faculty of Civil Engineering, Brno 602 00 CZ (phone: +420-541147382; fax: +420-541147392; e-mail: kala.z@fce.vutbr.cz)

Martin Kalina is with the Brno University of Technology, Faculty of Civil Engineering, Brno 602 00 CZ (phone: +420-541147131, e-mail: kalina.m1@fce.vutbr.cz).

The potential energy of three types of steep von Mises trusses was studied. The method form finding was also applied to the von Mises trusses with initial geometrical imperfections of axes of bars. The paper describes nonlinear phenomena present not only in beam structures [27], but also in thin-walled steel plates [28] or slender rock blocks [29]. The SES found on the energetic area can be divided into the points with minimum potential energy (stable SES), the points with maximum potential energy (unstable SES), and the points where mutual transition takes place (bifurcation points).

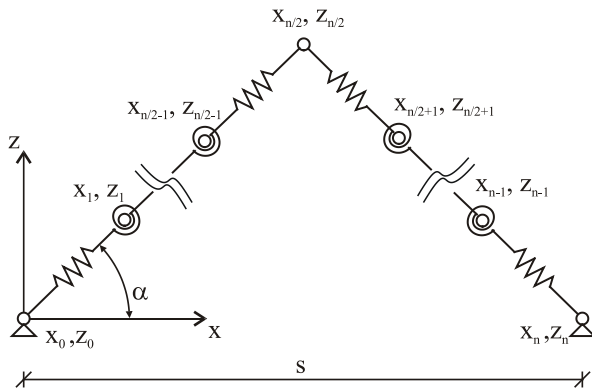


Fig. 2 model of von Mises planar truss

II. FORM FINDING METHOD

The potential energy storage in members of mechanical systems occurs when they are deformed, if forces are applied to the system [30]. A well-known elastic component is a coiled spring. The elastic behavior of springs and potential energy per unit volume can be found in [31].

In Fig. 2, there is the scheme of the discrete model of the von Mises truss consisting of parts of axial springs which allow the beams to compress or stretch, and of parts of coil springs which enable bending on the planes X and Z. The calculation of internal forces in coil springs  $F_l$  and coil springs  $M_\varphi$  is determined as, see [24].

$$F_l = k_l \cdot d_l, \quad M_\varphi = k_\varphi \cdot d_\varphi \tag{1}$$

where  $k_l$  is stiffness of axial spring (spring constant),  $d_l$  is the change of length (beam elongation or shortening) of axial spring,  $k_\varphi$  is stiffness of coil spring, and  $d_\varphi$ , angular change (rotation) of the coil spring. Within a certain range of deformation (rotations),  $k_l$  ( $k_\varphi$ ) remains constant and is defined as the negative ratio of displacement (rotation) to the magnitude of the restoring force (moment) produced by the axial spring (coil spring) at that displacement (rotation).

Elastic potential energy is one of the types of mechanical energy, which an elastic body has at its elastic deformation (stretch, compression, bending, torsion). The potential energy stored in axial spring is illustrated in Fig. 3. The potential energy stored in coil spring is presented in Fig. 4.

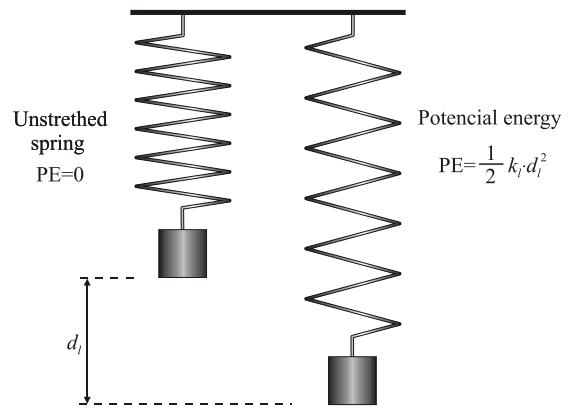


Fig. 3 potential energy of axial spring

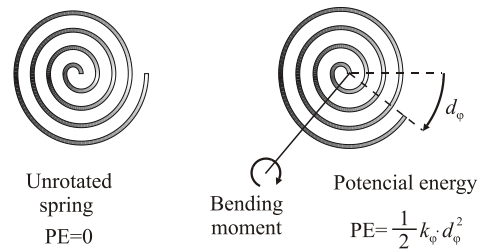


Fig. 4 potential energy of coil spring

The calculation of potential energy stored in the structure presented in Fig. 2 in axial springs and coil springs is determined as

$$PE = \frac{1}{2} \left( k_l \sum_{i=1}^{n_l} d_{li}^2 + k_\varphi \sum_{i=1}^{n_\varphi} d_{\varphi i}^2 \right) \tag{2}$$

where  $n_l$  is the number of axial springs, and  $n_\varphi$ , the number of coil springs. The position of each node is determined using the coordinate  $(x_i, z_i)$ , where  $i$  represents the index number of the node. The following equation will be used to calculate the length change of the axial spring:

$$d_{li} = l_i - l, \quad l_i = \sqrt{(x_{i+1} - x_i)^2 + (z_{i+1} - z_i)^2} \tag{3}$$

where  $l$  is original length of axial spring,  $l_i$  is length of axial spring after deformation of the von Mises truss. To calculate the angular change of coil spring,

$$d_{\varphi i} = \varphi_{i+1} - \varphi_i, \quad \tan \varphi_i = \frac{z_{i+1} - z_i}{x_{i+1} - x_i} \tag{4}$$

will be used where  $\varphi_i$  is the angular change of coil spring  $i$  (axial spring between the nodes (nodes  $i$  and  $i+1$ )). The asymmetry is introduced to the von Mises truss in the form of initial curvature of the left bar. The curvature shape is one half-wave of the function sinus (5).

$$w(x) = A \cdot \sin\left(\frac{\pi x}{L}\right) \quad (5)$$

where  $A$  is the amplitude of one half-wave of function sinus,  $L$  is the bar length. The von Mises trusses with asymmetry calculation are provided, in initial shape, with initial geometrical imperfection, so that their initial stress state is equal to zero stress.

To find SES of the von Mises truss, this nonlinear problem was solved by the method form finding.

$$\begin{aligned} \frac{\partial x_i}{\partial t} &= v_{xi}, \quad \frac{\partial v_{xi}}{\partial t} = \frac{1}{m} (R_{xi} - cv_{xi}) \\ \frac{\partial z_i}{\partial t} &= v_{zi}, \quad \frac{\partial v_{zi}}{\partial t} = \frac{1}{m} (R_{zi} - cv_{zi}) \end{aligned} \quad (6)$$

A dynamical calculation method is concerned, where the results depend on the choice of linear viscous damping force  $c$  acting on the joints. The mass  $m$  of the left or right bar is concentrated in individual nodes,  $v_{xi}$  and  $v_{yi}$  are the velocity vector components of the nodes, and  $R_{xi}$  and  $R_{zi}$  are the vector components of the resultant force  $R_i$  by which the springs act on the node. This system is solved by the Symplectic Euler method [32], which was generated by rearrangement of the explicite Euler method.

### III. SEARCH FOR SES

The model of the von Mises truss will be loaded by control displacement  $u$  at the point of top joint, i.e., in the coordinate  $x_{n/2}=s/2$ ,  $z_n/2$ . Before each control displacement, the von Mises truss persists for a certain relaxation time  $t_{rel}$ . After expiring of this time, the von Mises truss reaches SES, and the potential energy (PE) of the system is recorded.

The PE begins to be evaluated starting at the point of top joint in initial shape of the von Mises truss. As soon as PE has been recorded, the top joint displaces by control displacement  $u$  in direction of axis  $x$ . This step is repeated, until the top joint in coordinate  $x$  reaches the value of length  $L$  of one bar. After, the decrease of top joint takes place by control displacement  $u$ , and the top joint displaces by control displacement along the trajectory parallel with the foregoing path opposite the positive direction of coordinate  $x$ . The number of steps of control displacement opposite the direction of coordinate  $x$  is the same as the number of steps of control displacement in the direction of coordinate  $x$ , i.e., as soon as the top joint has reached the  $x$ -coordinate in the point of top joint of original state  $s/2$ , drop of top joint by control displacement  $u$  takes place again. This cycle is repeated, until the top joint approximates to the point of fixed bearing by means of control displacement, thus,  $x=s$ ,  $z=0$ . The whole process is schematically illustrated in Fig. 5.

The PE of the system is recorded before each control displacement  $u$ .

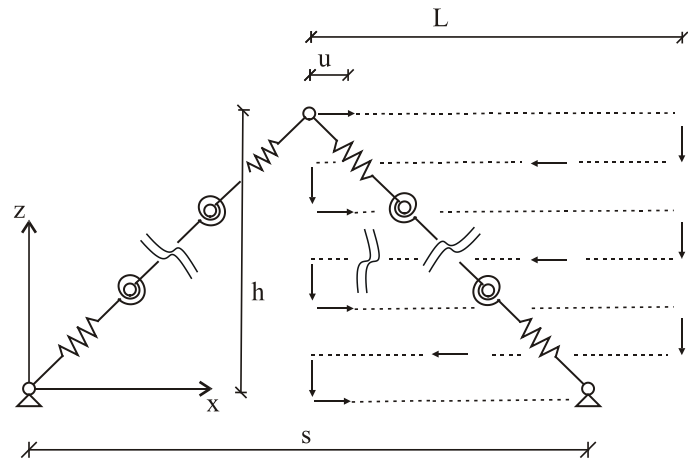


Fig. 5 description of shifting of top hinge

To present the SES area, the PE was transformed into the nondimensional quantity

$$PE_r = \frac{PE}{PE_{s/2}} \quad (7)$$

where PE is the potential energy of the system at any horizontal displacement of top joint in the coordinate raster  $x$ , and corresponding to relevant  $z$ -coordinate,  $PE_{s/2}$  is the value of potential energy of the system for the top joint localized in the half span of the von Mises truss corresponding to relevant  $z$ -coordinate.

### IV. DESCRIPTION OF POTENTIAL ENERGY

SES were obtained on steep von Mises trusses with angle  $\alpha = 45^\circ$ ,  $\alpha = 55^\circ$  a  $\alpha = 60^\circ$ . For each von Mises truss of this type, SES were calculated with influence of initial geometrical imperfection and without the influence of that imperfection. To highlight the influence of imperfection in graphic illustration, the design of size of its amplitude  $A = 0.1$  m does not correspond with the real state which is usually considered as the thousandth of bar length, see, e.g., [11-13]. In the calculation model, cross-section characteristics of European steel hot-rolled cross-section IPE400 were considered for each bar: cross-section area is  $8446 \text{ mm}^2$ , second moment of area about minor axis is  $231.3 \cdot 10^{-6} \text{ m}^4$ , and Young's modulus is  $210 \text{ GPa}$ .

The chosen relaxation time is  $t_{rel} = 10 \text{ s}$  at the time step  $t_{step} = 10^{-4} \text{ s}$  and damping coefficient  $c = 100 \text{ kNs/m}$ . The size of a step of one displacement was chosen  $u = 0.02 \text{ m}$ . The mapping of potential energy proceeds within the tetragonal raster  $Lxh$ , as it was presented in Fig. 5. First, the right side of the values of potential energy is obtained, and after, the bars are swapped, and so, the left part of values of potential energies is obtained. The modern application MapPoEng [33] deals with investigation into potential energy, as well.

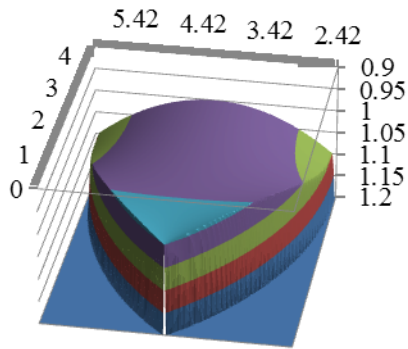


Fig. 6  $PE_T$  for  $\alpha = 45^\circ$  without imperfection

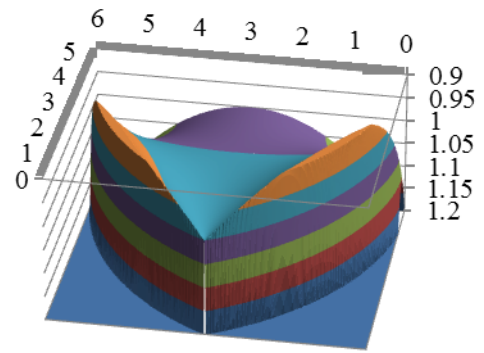


Fig. 10  $PE_T$  for  $\alpha = 60^\circ$  without imperfection

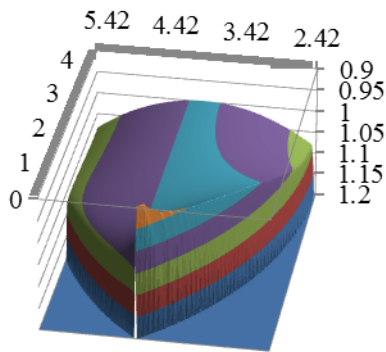


Fig. 7  $PE_T$  for  $\alpha = 45^\circ$  with imperfection

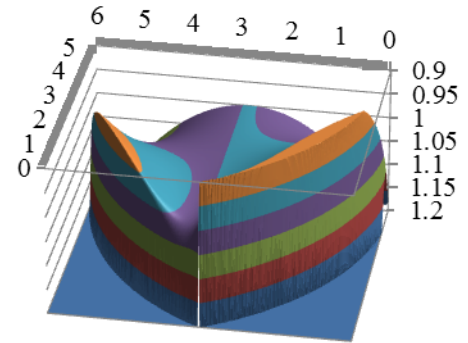


Fig. 11  $PE_T$  for  $\alpha = 60^\circ$  with imperfection

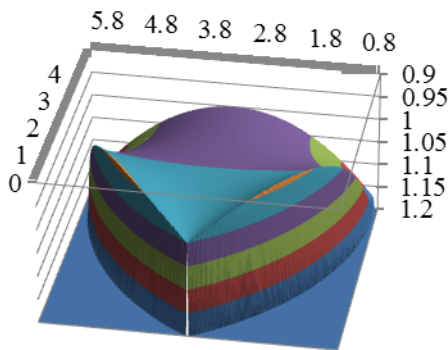


Fig. 8  $PE_T$  for  $\alpha = 55^\circ$  without imperfection

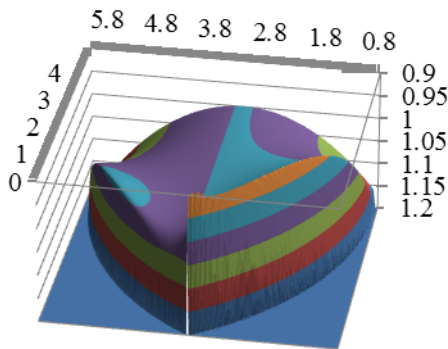


Fig. 9  $PE_T$  for  $\alpha = 55^\circ$  with imperfection

The resulting values of potential energies are transposed to nondimensional numbers according to (7), applying transformation. This step was carried out because of clearness of resulting graphic areas. These areas can be seen in Fig. 6 to Fig. 11. The position of top joint of the von Mises truss has its coordinates  $Coord.z = 0$ ;  $Coord.x = s/2$ . The values of transformed potential energy  $PE_T$  are given by the vertical axis. For the clearness' sake, the values of transformed potential energy are presented within the interval (0.9; 1.2). The Figures show how the SES gets changed at increasing height  $h$ . It can be seen that, by introducing the imperfection to the models, this asymmetry manifests itself even in the area of transformed potential energy, and that the same asymmetry has higher influence on the stability of the von Mises truss at larger height  $h$ .

### V. CONCLUSION

The presented paper describes the method of analysis of the stability of steep von Mises trusses. Areas of potential energy of three types of steep von Mises trusses were calculated, based on the method mentioned. It can be concluded from these areas that the height (steepness) of the von Mises truss influences statical equilibrium states. The interesting share concerning the influence of these states belongs also to the chosen geometrical imperfection of one bar for all types of the von Mises trusses. It became evident that the following problem is worthy of investigation saying whether the size of geometrical imperfection can influence also SES of low von Mises trusses.

Elastic potential energy in mechanical systems is a very precious indicator of stability or instability of a structure. Energy storage in elastic deformations in the mechanical domain offers an alternative to the electrical, electrochemical, chemical, and thermal energy storage approaches [30]. The presented areas of transformed potential energy have clearly shown how it is appropriate to apply them to investigation into the stability and bifurcation points of nonlinear systems.

## ACKNOWLEDGMENT

This result was achieved with the financial support of the projects GAČR 14 17997S and LO1408 “AdMAs UP”.

## REFERENCES

- [1] R. von Mises, “Über die Stabilitätsprobleme der Elastizitätstheorie,” *ZAMM* 3, pp. 2107-2110, 1923.
- [2] R. von Mises, J. Ratzersdorfer, “Die Knicksicherheit von Fachwerken,” *ZAMM* 5, pp. 218-235, 1925.
- [3] T. V. Galambos, *Stability Design Criteria for Metal Structures*. John Wiley and Sons, Ltd., 1998, p. 911.
- [4] M. Kalina, “Static Task of von Mises Planar Truss Analyzed using Potential Energy,” *AIP Conference Proceedings*, vol. 1558, pp. 2107-2110, 2013.
- [5] S.P. Timoshenko, J. Gere, *Theory of elastic stability*, McGraw Hill New York, 1961.
- [6] I. Vayas, “Lateral torsional buckling of girders with monosymmetric cross-sections,” *Stahlbau*, vol. 73, pp. 107-115, 2004.
- [7] T. V. Galambos, *Stability Design Criteria for Metal Structures*. John Wiley and Sons, Ltd., 1998, p. 911.
- [8] L.H. Teh, B.P. Gilbert, “A buckling model for the stability design of steel columns with intermediate gravity loads,” *Journal of Constructional Steel Research*, vol. 117, pp. 243–254, 2016.
- [9] M. Štrba, M. Karmazínová, “The development and testing of a new type of the temporary steel truss footbridge with closed cross-section,” *International Journal of Mechanics*, vol. 9, pp. 173–180, 2015.
- [10] M. Karmazínová, J. Melcher, “Initial imperfections of steel and steel-concrete composite columns subjected to buckling compression,” *WSEAS Transactions on Applied and Theoretical Mechanics*, vol. 9, pp. 27-34, 2014.
- [11] Z. Kala, J. Kala, “Sensitivity analysis of stability problems of steel structures using shell finite elements and nonlinear computation methods,” *WSEAS Transactions on Applied and Theoretical Mechanics*, vol. 4, no. 3, pp. 105–114, 2009.
- [12] Z. Kala, “Sensitivity and reliability analyses of lateral-torsional buckling resistance of steel beams,” *Archives of Civil and Mechanical Engineering*, vol. 15, no. 4, pp. 1098–1107, 2015.
- [13] M. Kala, “Global sensitivity analysis in stability problems of steel frame structures,” *Journal of Civil Engineering and Management*, vol. 22, no. 3, pp. 417–424, 2016.
- [14] Z. Kala, J. Kala, and A. Omishore, “Probabilistic Buckling Analysis of Thin-Walled Steel Columns Using Shell Finite Elements,” *International Journal of Mechanics*, vol. 10, pp. 213–218, 2016.
- [15] Z. Kala, “Reliability analysis of the lateral torsional buckling resistance and the ultimate limit state of steel beams with random imperfections,” *Journal of Civil Engineering and Management*, vol. 21, no. 7, pp. 902–911, 2015.
- [16] A. Omishore, “Uncertainty analysis of the cross-sectional area of a structural member,” in *Proc. of the 4th WSEAS Int. Conf. on EMESEG'11*, Corfu, 2011, pp. 284–288.
- [17] J. Antucheviciene, Z. Kala, M. Marzouk, E.R. Vaidogas, “Solving civil engineering problems by means of fuzzy and stochastic MCDM methods: Current state and future research,” *Mathematical Problems in Engineering*, vol. 2015, Article ID 362579, p. 16, 2015.
- [18] J. Antucheviciene, Z. Kala, M. Marzouk, E.R. Vaidogas, “Decision making methods and applications in civil engineering,” *Mathematical Problems in Engineering*, vol. 2015, Article ID 160569, p. 3, 2015.
- [19] F. Baño, Á. Mena, F. Viscaino, J. Rubio, G. Rodríguez-Bárcenas, “Metaheuristic algorithms helping to take decisions in investment portfolios,” *Archives of Civil and Mechanical Engineering*, vol. 4, pp. 19–24, 2016.
- [20] E. Castillo, J.A. Lozano-Galant, M. Nogal, J. Turmo, “New tool to help decision making in civil engineering,” *Journal of Civil Engineering and Management*, vol. 21, no. 6, pp. 689–697, 2015.
- [21] D.B. Hammad, N. Shafiq and M. F. Nuruddin, “Criticality index of building systems using multi-criteria decision analysis technique,” *MATEC Web of Conferences*, vol. 15, Article 01018, p. 7, 2014.
- [22] M. Medineckiene, E.K. Zavadskas, F. Björk, Z. Turskis, “Multi-criteria decision-making system for sustainable building assessment/certification,” *Archives of Civil and Mechanical Engineering*, vol. 15, no. 1, pp. 11–18, 2015.
- [23] O. Sucharda, J. Vasek, J. Kubosek, “Elastic-Plastic calculation of a steel beam by the finite element method,” *International Journal of Mechanics*, vol. 9, pp. 228–235, 2015.
- [24] P. Frantík, “Simulation of the stability loss of the von Mises truss in an unsymmetrical stress state,” *Journal Engineering Mechanics*, vol. 14, pp. 155-162, 2007.
- [25] L. Kwasniewski, “Complete equilibrium paths for Mises trusses,” *International Journal of Non-Linear Mechanics* 44(1), pp. 19-26, 2009.
- [26] V. Zakovorotny, “Bifurcation in the dynamic system of the mechanic processing in metal-cutting tools,” *WSEAS Transactions on Applied and Theoretical Mechanics*, vol. 10, pp. 102-116, 2015.
- [27] A. Omishore, “Verification of Design Procedures of Structural Stability using Probabilistic Methods of Reliability Analysis,” *AIP Conference Proceedings*, vol. 1479, no. 1, pp. 2082-2085, 2012.
- [28] J. Ravinger, M. Psotný, “Stable nad unstable paths in the post-buckling behaviour of slender web,” *Proceedings of the Fourth International Conference on Coupled Instabilities in Metal Structures*, Rome, (Italy), pp. 67-75, 2004.
- [29] Ch. Mathey, C. Feau, I. Politopoulos, D. Clair, L. Baillet and M. Fogli, “Experimental and numerical response of rigid slender blocks with geometrical defects under seismic excitation,” *MATEC Web of Conferences*, vol. 24, Article number 09004, p. 7, 2014.
- [30] F. Rossi, B. Castellani, A. Nicolini, “Benefits and challenges of mechanical spring systems for energy storage applications,” *Energy Procedia*, vol. 82, pp. 805-810, 2015.
- [31] F.A. Hill, T.F. Havel, D. Lashmore, M. Schauer, C. Livermore, “Storing energy and powering small systems with mechanical springs made of carbon nanotube yarn,” *Energy* 76, pp. 318-325, 2014.
- [32] E. Hairer, Ch. Lubich, G. Wanner, “Geometric Numerical Integration illustrated by the Störmer/Verlet method,” *Acta Numerica*, vol. 12, pp. 339-450, 2003.
- [33] P Frantík, “MapPoEng: Mapping of Potential Energy,” 2015, Software available at <http://mappoeng.kitnarf.cz>